
A BLACKBOX YIELD ESTIMATION WORKFLOW WITH GAUSSIAN PROCESS REGRESSION FOR INDUSTRIAL PROBLEMS

Mona Fuhrländer^{1,2}, Sebastian Schöps^{1,2}

¹ Computational Electromagnetics Group, Technische Universität Darmstadt, Germany

² Centre for Computational Engineering, Technische Universität Darmstadt, Germany

ABSTRACT

In this paper an efficient and reliable method for stochastic yield estimation is presented. Since one main challenge of uncertainty quantification is the computational feasibility, we propose a hybrid approach where most of the Monte Carlo sample points are evaluated with a surrogate model, and only a few sample points are reevaluated with the original high fidelity model. Gaussian Process Regression is a non-intrusive method which is used to build the surrogate model. Without many prerequisites, this gives us not only an approximation of the function value, but also an error indicator that we can use to decide whether a sample point should be reevaluated or not.

Keywords Yield Analysis, Failure Probability, Uncertainty quantification, Monte Carlo, Gaussian Process Regression, Surrogate Model, Blackbox

1 Introduction

In mass production of devices, e.g. antennas or filters, often one has to deal with uncertainties in the manufacturing process. These uncertainties may lead to deviations in important parameters, e.g. geometrical or material parameters. Those may lead to rejections due to malfunctioning. In this context, the quantification of uncertainty and its impact plays an important role, also with regard to later optimization. According to Graeb [1, Chap. 2] we define the yield as the percentage of realizations in a manufacturing process, which fulfills performance feature specifications. When dealing with electromagnetism, the performance feature specifications require to solve partial differential equations (PDE), e.g., with the finite element method (FEM). The most straightforward approach for yield estimation is the Monte Carlo (MC) analysis [2, Chap. 5], which requires typically many evaluations of the underlying PDEs. Thus, the computational effort is one main challenge of yield estimation.

Over the last decades, various methods have been developed with the aim of reducing the computational effort of MC. One approach to achieve this is to reduce the number of sample points, e.g. by Importance Sampling (IS) [2, Chap. 5.4]. Another approach is to reduce the effort for each sample point, e.g. by using surrogate based approaches [3, 4, 5]. The cost for building most surrogate models increases rapidly with the number of uncertain parameters. Furthermore, there are counter examples where the yield estimator fails drastically, even though the surrogate model seems highly accurate, measured by classical norms or pointwise [6]. Therefore the same authors propose a hybrid approach. They focus their attention on critical sample points that are close to the limit state function, which is the limit between sample points fulfilling and not fulfilling the performance feature specifications. Critical sample points are evaluated on the original high-fidelity model, while the other sample points that are far from the limit state function are evaluated only on a surrogate model. Here, the choice of the surrogate model and the definition of *close* and *far* are crucial. In [7], a hybrid approach is proposed, using radial basis functions (RBF) for the surrogate model and an adjoint error indicator to choose the critical sample points. In [8] a similar hybrid approach is proposed, using stochastic collocation with polynomial basis functions and also an adjoint error indicator. In this paper we combine these ideas and propose a hybrid approach using Gaussian Process Regression (GPR) for both, building the surrogate model and obtaining an error indicator in form of the prediction variance given by the GPR. Further, a part of the critical sample points is used to improve the GPR model adaptively during the estimation process.

Other research related to GPR based surrogate models for yield or failure probability estimation is conducted in [9, 10, 11]. In [9], the authors concentrate on the calculation of small failure probabilities with a limited number of function

evaluations on the original model. They also use an adaptive GPR surrogate model, but do not combine it with a hybrid approach and therefore have no critical sample points that could be used to improve the GPR model. Instead, they distinguish between the sample points generated by Subset Simulation (Sequential MC) for error probability estimation and those generated as training data using a Stepwise Uncertainty Reduction technique to refine the GPR model adaptively. In [10] and [11], a GPR based surrogate model approach is combined with IS. Again, no hybrid approach is used. Adaptively, GPR model and IS density are improved by adding one or more sample points from the MC sample of the last iteration to the training data set, which are selected by a learning function and then calculated on the original model. On the contrary, in practice it is often assumed that the design parameter deviations are small in a way that a linearization is valid [12, Online Help: Yield Analysis Overview]. This approach is obviously very efficient but it is very difficult to determine on beforehand if the assumption is valid.

The paper is structured as follows. After setting up the problem, in Section 3 existing approaches and the concept of GPR are briefly described. Then the use of GPR for yield estimation, also in combination with a hybrid approach, is discussed. In Section 4, numerical results are presented using a benchmark problem, a simple waveguide, and a practical example, a low pass filter calculated with CST, before the paper is concluded in Section 5.

2 Problem Setting

We will focus on problems from the electrical engineering industry but the ideas are very generally applicable. Let \mathbf{p} denote a vector of design parameters. Starting from Maxwell's formulation of the electric field

$$\nabla \times (\mu^{-1} \nabla \times \mathbf{E}_\omega) - \omega^2 \epsilon \mathbf{E}_\omega = j\omega \mathbf{J} \quad \text{on } D,$$

where $\mathbf{E}_\omega = \mathbf{E}_\omega(\mathbf{x}, \mathbf{p})$ denotes the electric field phasor, ω the angular frequency, $\mu = \mu_r \mu_0$ the dispersive complex magnetic permeability, $\epsilon = \epsilon_r \epsilon_0$ the dispersive complex electric permittivity and $\mathbf{J} = \mathbf{J}(\mathbf{x}, \mathbf{p})$ the phasor of current density. The vacuum and relative permeability are denoted by μ_0 and $\mu_r = \mu_r(\mathbf{x}, \mathbf{p})$, the vacuum and relative permittivity respectively by ϵ_0 and $\epsilon_r = \epsilon_r(\mathbf{x}, \mathbf{p})$. Assuming suitable boundary conditions, building the weak formulation and discretizing with (high-order) Nédélec basis functions we derive the linear system

$$\mathbf{A}_\omega(\mathbf{p}) \mathbf{e}_\omega(\mathbf{p}) = \mathbf{f}_\omega, \quad (1)$$

with system matrix $\mathbf{A}_\omega(\mathbf{p})$, discrete solution $\mathbf{e}_\omega(\mathbf{p})$, the discretized right-hand side \mathbf{f}_ω , all depending on the design parameter \mathbf{p} and the frequency ω . For further details we refer to [13, 14, 15]. As quantity of interest (QoI)

$$Q_\omega(\mathbf{p}) = q(\mathbf{e}_\omega(\mathbf{p})),$$

we consider the scattering parameter (S-parameter), i.e. $Q_\omega(\mathbf{p}) := S_\omega(\mathbf{p})$. In this case, q is an affine linear function.

If there are uncertainties in the manufacturing process, the design parameters may be subject to random deviations. Therefore we model the uncertain parameter vector \mathbf{p} as multidimensional random variable. We assume \mathbf{p} to be (truncated) Gaussian distributed (cf. [16]), i.e. $\mathbf{p} \sim \mathcal{N}_{\mathcal{T}}(\bar{\mathbf{p}}, \Sigma, \mathbf{lb}, \mathbf{ub})$ with mean value $\bar{\mathbf{p}}$, covariance matrix Σ , lower and upper bounds \mathbf{lb} and \mathbf{ub} and a probability density function $\text{pdf}(\mathbf{p})$. Other distributions are also possible. Following [1] we define the performance feature specifications as a restriction on our QoI in a specific interval, i.e.

$$|S_\omega(\mathbf{p})| \leq c \quad \forall \omega \in T_\omega = [\omega_l, \omega_u] \text{ in GHz}, \quad (2)$$

where c is a constant and ω the range parameter defined in the frequency domain. The safe domain is defined as the set containing all parameters, fulfilling the performance feature specifications, i.e.

$$\Omega_s := \{\mathbf{p} : |S_\omega(\mathbf{p})| \leq c \quad \forall \omega \in T_\omega\}.$$

Then, the yield can be written as [1, Chap. 4.8.3, Eq. (137)]

$$Y(\bar{\mathbf{p}}) := \mathbb{E}[\mathbf{1}_{\Omega_s}(\mathbf{p})] := \int_{-\infty}^{\infty} \cdots \int_{-\infty}^{\infty} \mathbf{1}_{\Omega_s}(\mathbf{p}) \text{pdf}(\mathbf{p}) \, d\mathbf{p},$$

where \mathbb{E} denotes the expected value and $\mathbf{1}_{\Omega_s}$ the indicator function with value 1 if the parameter \mathbf{p} lies inside the safe domain and value 0 otherwise.

3 A GPR-Hybrid Approach for Yield Estimation

In a MC analysis a large number of sample points is generated, according to the truncated normal distribution of the uncertain parameters, and evaluated in order to obtain the QoI. The fraction of sample points lying inside the safe

domain is an estimator for the yield. Since the accuracy depends directly on the size of the sample, a classic MC analysis comes with high computational costs [17]. The stochastic collocation hybrid approach proposed by [8] showed that the computational effort can be reduced significantly while ensuring the same accuracy and robustness as with a classic MC method. Nevertheless, there are a few drawbacks. First, since a polynomial collocation approach was used, the training data for the surrogate model must come from a tensorial grid and cannot be chosen arbitrarily. As a consequence the surrogate model cannot be updated easily, e.g. with the information from the evaluation of critical sample points. This could be handled by using regression, but the second disadvantage would still remain: In order to distinguish between critical and non-critical sample points an adjoint error indicator was used. This requires the system matrices and the solution of the primal and the dual problem, which is not always given when using proprietary software. The GPR-Hybrid approach we propose in this paper overcomes these issues.

3.1 Gaussian Process Regression

Following Rasmussen and Williams [4, Chap. 2.2], the technique of Gaussian Process Regression can be divided into four mandatory steps and one optional step.

1. Prior: We make some prior assumptions about the functions we expect to observe. We write

$$(S_{\mathbf{p}})_{\mathbf{p} \in \mathbf{P}} \sim \mathcal{GP}(m(\mathbf{p}), k(\mathbf{p}, \mathbf{p}')),$$

if we expect the S-parameter to follow a Gaussian Process (GP) with specific mean m and kernel function k . In the following we use the constant zero function as a starting value for the mean function and choose the squared exponential kernel function, which is also known as RBF, i.e.

$$k(\mathbf{p}, \mathbf{p}') = \zeta e^{-\frac{|\mathbf{p} - \mathbf{p}'|^2}{2l^2}},$$

with the two hyperparameters $\zeta \in \mathbb{R}$ and $l > 0$. At this point we refer to Section 4 to see how we set the hyperparameters. For more information about hyperparameters in general, please refer to [4, Chap. 5].

2. Training data: We collect data by evaluating sample points on the original FE model. The so-called training data set

$$\mathcal{T} = \{\mathbf{P} = [\mathbf{p}_1, \dots, \mathbf{p}_n], \mathbf{S} = [S(\mathbf{p}_1), \dots, S(\mathbf{p}_n)]\}$$

will be used to train the GP.

3. Posterior: In this step the information from the prior and the training data is combined in order to obtain a new GP, with updated mean and kernel function. We write

$$\mathbf{K} = \begin{bmatrix} k(\mathbf{p}_1, \mathbf{p}_1) & \dots & k(\mathbf{p}_1, \mathbf{p}_n) \\ \vdots & & \vdots \\ k(\mathbf{p}_n, \mathbf{p}_1) & \dots & k(\mathbf{p}_n, \mathbf{p}_n) \end{bmatrix} \text{ and } \mathbf{m} = \begin{bmatrix} m(\mathbf{p}_1) \\ \vdots \\ m(\mathbf{p}_n) \end{bmatrix}, \quad (3)$$

then the posterior distribution of the output $S_{\mathbf{p}}$ depending on the training data set \mathcal{T} is given by

$$S_{\mathbf{p}} | \mathbf{P}, \mathbf{S} \sim \mathcal{N}(\mathbf{m}, \mathbf{K}).$$

4. Predictions: For an arbitrary test data point \mathbf{p}^* and a parametrization of ω , the predicted distribution of the output $S_{\mathbf{p}^*}$ depending on the training data set \mathcal{T} and the test data point is given by

$$S_{\mathbf{p}^*} | \mathbf{p}^*, \mathbf{P}, \mathbf{S} \sim \mathcal{N}(m(\mathbf{p}^*) + \mathbf{k}(\mathbf{p}^*, \mathbf{P})\mathbf{K}^{-1}(\mathbf{S} - \mathbf{m}), \\ k(\mathbf{p}^*, \mathbf{p}^*) - \mathbf{k}(\mathbf{p}^*, \mathbf{P})\mathbf{K}^{-1}\mathbf{k}(\mathbf{P}, \mathbf{p}^*)), \quad (4)$$

with

$$\mathbf{k}(\mathbf{p}^*, \mathbf{P}) = [k(\mathbf{p}^*, \mathbf{p}_1), \dots, k(\mathbf{p}^*, \mathbf{p}_n)], \\ \mathbf{k}(\mathbf{P}, \mathbf{p}^*) = [k(\mathbf{p}_1, \mathbf{p}^*), \dots, k(\mathbf{p}_n, \mathbf{p}^*)]^T.$$

Thus, predictions of the function value $\tilde{S}_{\omega}(\mathbf{p}^*)$ and the variance $\sigma_{\omega}(\mathbf{p}^*)$ can be obtained. Please note, that the kernel function of the GPR is a measure for accuracy of the surrogate model and is not related to the design uncertainty.

5. Model update (optional): A new data point $(\mathbf{p}_{\text{add.}}, S(\mathbf{p}_{\text{add.}}))$ can be used to update an existing GPR model. Therefore the training data set is updated to

$$\mathbf{P}_{\text{new}} = [\mathbf{P}, \mathbf{p}_{\text{add.}}] \text{ and } \mathbf{S}_{\text{new}} = [\mathbf{S}, S(\mathbf{p}_{\text{add.}})], \quad (5)$$

as well as (3) has to be updated according to

$$\mathbf{K}_{\text{new}} = \begin{bmatrix} \mathbf{K} & \mathbf{k}(\mathbf{P}, \mathbf{p}_{\text{add.}}) \\ \mathbf{k}(\mathbf{p}_{\text{add.}}, \mathbf{P}) & k(\mathbf{p}_{\text{add.}}, \mathbf{p}_{\text{add.}}) \end{bmatrix} \text{ and } \mathbf{m}_{\text{new}} = \begin{bmatrix} \mathbf{m} \\ m(\mathbf{p}_{\text{add.}}) \end{bmatrix}. \quad (6)$$

Then, predictions for a new test data point \mathbf{p}^* can be obtained by (4) using the updated data from (5) and (6). Thus, the main part of the computational effort when updating the GPR model is the inversion of the matrix \mathbf{K}_{new} . For more detailed information about GPR we refer to [4, Chap. 2].

3.2 Combining GPR and the Hybrid Approach

The idea of the hybrid approach is saving computing time by evaluating most of the MC sample points on a cheap to evaluate surrogate model and only a small subset of the sample on the original high fidelity (e.g. FE) model. The sample points evaluated on the original model are called critical sample points. As mentioned before, the choice of the critical sample points is crucial, for efficiency and accuracy of this approach. In [7] and [8] adjoint error indicators are used. Here, we take advantage of the GPR that provides an error indicator point \mathbf{p} in the form of the variance $\sigma_\omega(\mathbf{p})$. Algorithm 1 shows the classification procedure for one sample point \mathbf{p}_i . The performance feature specification expects

Algorithm 1 Hybrid decision

```

1: Input: sample point  $\mathbf{p}_i$ , frequency range  $T_d$ , threshold  $c$ , safety factor  $\gamma$ , GPR surrogate models
2: for  $j = 1, \dots, |T_d|$  do
3:   Evaluate the GPR model and obtain  $\tilde{S}_{\omega_j}(\mathbf{p}_i)$  and  $\sigma_{\omega_j}(\mathbf{p}_i)$ 
4:   if  $|\tilde{S}_{\omega_j}(\mathbf{p}_i)| + \gamma |\sigma_{\omega_j}(\mathbf{p}_i)| \leq c$  then
5:     Classify  $\mathbf{p}_i \in \Omega_s$  (accepted) and continue with  $j = j + 1$ 
6:   else if  $|\tilde{S}_{\omega_j}(\mathbf{p}_i)| - \gamma |\sigma_{\omega_j}(\mathbf{p}_i)| > c$  then
7:     Classify  $\mathbf{p}_i \notin \Omega_s$  (not accepted) and stop
8:   else
9:     Evaluate the original model and obtain  $S_{\omega_j}(\mathbf{p}_i)$ 
10:    if  $|S_{\omega_j}(\mathbf{p}_i)| \leq c$  then
11:      Classify  $\mathbf{p}_i \in \Omega_s$  (accepted) and continue with  $j = j + 1$ 
12:    else
13:      Classify  $\mathbf{p}_i \notin \Omega_s$  (not accepted) and stop
14:    end if
15:  end if
16: end for

```

the inequality (2) to hold in the whole frequency interval T_ω . However, we define a discrete subset $T_d \subset T_\omega$ and enforce only that the inequality holds for all $\omega_j \in T_d$. This means, for each frequency point ω_j a separate surrogate model is built, otherwise rational interpolation can be used, e.g. [18]. Further, we build separate surrogate models for the real part and the imaginary part of the S-parameter, and later combine them for the prediction. This guarantees (affin-)linearity of the QoI by avoiding the square root. Once the GPR models are constructed, a MC analysis is carried out on the surrogates. For each sample point a predicted S-parameter value and a predicted variance are obtained. The predicted variance multiplied with a safety factor γ serves as a buffer zone. If the performance feature specification (2) is (not) fulfilled for the predicted S-parameter value and all values in the range plus/minus this buffer zone the considered sample point is classified as (not) accepted, else it is classified as critical and reevaluated on the original model. Then, the yield will be estimated by

$$\tilde{Y}(\bar{\mathbf{p}}) = \frac{1}{N_{\text{MC}}} \sum_{i=1}^{N_{\text{MC}}} \mathbf{1}_{\Omega_s}(\mathbf{p}_i),$$

where N_{MC} is the size of the MC sample. A significant advantage of GPR is, that the model can be easily updated on the fly. Algorithm 2 shows the process of yield estimation including updating the GPR models. Typically the computational effort of a surrogate based approach lies in the *offline* evaluation of the training data. Therefore we start with a small initial training data set. The resulting less accurate GPR model does not pose a problem in terms of yield estimation

Algorithm 2 Yield Estimation with GPR

```

1: Input: initial GPR models for each frequency point  $\omega_j \in T_d$ , set of MC sample points  $\mathbf{p}_i, i = 1, \dots, N_{MC}$ , error
   tolerance  $\varepsilon_t > 0$ , integer divisor  $N_{update}$  of  $N_{MC}$ 
2: for  $i = 1, \dots, N_{MC}$  do
3:   Classify  $\mathbf{p}_i$  according to Algorithm 1
4:   for  $j = 1, \dots, |T_d|$  do
5:     Define  $\mathcal{C}_j = \{\mathbf{p}_i : \mathbf{p}_i \text{ classified as critical for } \omega_j \text{ in last } N_{update} \text{ MC evaluations}\}$ 
6:   end for
7:   if  $i$  integer multiplier of  $N_{update}$  then
8:     for  $j = 1, \dots, |T_d|$  do
9:       Initialize  $\varepsilon = \varepsilon_t + 1$ 
10:      while  $\varepsilon > \varepsilon_t$  do
11:        Set  $\mathbf{p}_{add} = \arg \max_{\mathbf{p}_i \in \mathcal{C}_j} |\tilde{S}_{\omega_j}(\mathbf{p}_i) - S_{\omega_j}(\mathbf{p}_i)|$ 
12:        Update GPR model for  $\omega_j$  with sample point  $\mathbf{p}_{add}$ .
13:        Evaluate updated GPR model and obtain updated  $\tilde{S}_{\omega_j}(\mathbf{p}_i)$  for all  $\mathbf{p}_i \in \mathcal{C}_j$ 
14:        Calculate  $\varepsilon = \max_{\mathbf{p}_i \in \mathcal{C}_j} |\tilde{S}_{\omega_j}(\mathbf{p}_i) - S_{\omega_j}(\mathbf{p}_i)|$ 
15:      end while
16:    end for
17:  end if
18: end for
19: Estimate the yield with  $Y(\bar{\mathbf{p}}) = \frac{|\Omega_s|}{N_{MC}}$ 

```

accuracy, because the hybrid method still classifies all sample points correctly. Then, during the estimation process (*online*), we use a part of the critical sample points to improve our GPR model. This requires almost no additional computational effort, since these sample points were calculated in the hybrid method anyway. Also, the computational effort to update the GPR model (see step 5 in Section 3.1) is negligible compared to the costs of FE model evaluations. The critical sample points which are added to the training data set are chosen in a greedy way: After a fixed number N_{update} of MC sample points is evaluated (possibly in parallel), the resulting critical sample points of the j -th frequency point are collected in the set \mathcal{C}_j . Then, the sample point for which the difference between the predicted value and the real value of the S-parameter is maximum will be included in the training data set. The GPR model is updated with the additional training data point and all sample points in \mathcal{C}_j are evaluated on the new GPR surrogate model in order to obtain a new prediction. This procedure is repeated until the error is below a tolerance ε_t . Then, the next N_{update} MC sample points are evaluated (in parallel), using the updated GPR model.

4 Numerical Results

In the following we perform numerical tests on two examples, a dielectrical waveguide and a stripline low pass filter. The results of the waveguide are also compared with the estimates resulting from a linearization, which is common in industry.

4.1 Dielectrical Waveguide

The benchmark problem on which we perform the numerical tests is a simple dielectrical waveguide, cf. [8]. We consider two uncertain geometrical parameters, the length of the dielectrical inlay p_1 , the length of the offset p_2 (see Figure 1), and two uncertain material parameters p_3 and p_4 with the following effect on the relative permeability and permittivity of the inlay

$$\begin{aligned}\epsilon_r &= 1 + p_3 + (1 - p_3) \left(1 + j\omega (2\pi 5 \cdot 10^9)^{-1}\right)^{-1}, \\ \mu_r &= 1 + p_4 + (2 - p_4) \left(1 + j\omega (1.1 \cdot 2\pi 20 \cdot 10^9)^{-1}\right)^{-1}.\end{aligned}$$

The mean and covariance (in mm) is given by

$$\bar{\mathbf{p}} = [10.36, 4.76, 0.58, 0.64]^T \text{ and } \Sigma = \text{diag}([0.7^2, 0.7^2, 0.3^2, 0.3^2]).$$

The distribution of the geometrical parameters is truncated on the left at $p_i - 3$ mm and on the right at $p_i + 3$ mm ($i = 1, 2$), the distribution of the material parameters is truncated on the left at $p_i - 0.3$ and on the right at $p_i + 0.3$

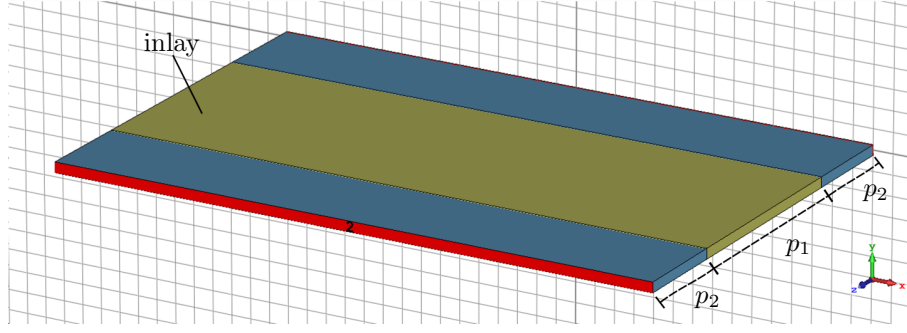


Figure 1: Rectangular waveguide with dielectrical inlay of length p_1 modelled in CST [12].

($i = 3, 4$). The performance feature specifications are

$$|S_\omega(\mathbf{p})| \stackrel{!}{\leq} -24 \text{ dB} \quad \forall \omega \in T_\omega = [2\pi 6.5, 2\pi 7.5] \text{ in GHz.}$$

In this frequency range we consider eleven equidistant frequency points $\omega_j \in T_d$. The size of the MC sample is set to $N_{MC} = 2,500$. According to

$$\sigma_Y = \sqrt{\frac{Y(\bar{\mathbf{p}})(1 - Y(\bar{\mathbf{p}}))}{N_{MC}}} \leq \frac{0.5}{\sqrt{N_{MC}}}, \quad (7)$$

where σ_Y denotes the standard deviation of the yield estimator, this gives us a standard deviation of the yield estimator of less than 0.01 for all possible sizes of the yield [17]. Further, we set the safety factor $\gamma = 2$, the error tolerance $\varepsilon_t = 0.01$ and the MC steps $N_{update} = 50$, which can be for example chosen according to the number of parallel processors available.

In order to build the GPR surrogate model, the python package scikit-learn has been used [19]. The applied kernel is the product of a constant kernel representing ζ and a RBF kernel representing the exponential function with hyperparameter l . In scikit-learn, the hyperparameters have a starting point, in our case $\zeta_0 = 0.1$ and $l_0 = 1$, and then they are optimized within given bounds, in our case $b_\zeta = (10^{-5}, 10^{-1})$ and $b_l = (10^{-5}, 10^5)$, respectively. We allowed a maximum of 10 iteration steps for the optimization of the hyperparameters and set the noise parameter $\alpha = 10^{-5}$, which is recommended to consider numerical issues, e.g. mesh noise. Once we have evaluated first training data points, the training data's mean is set as mean function of the GP.

For the simple waveguide a closed form solution of (1) exists, cf. [20]. However, we will refer to this solution as high fidelity solution in the following, since in practice a computational expensive FEM evaluation would be necessary at this point. The yield estimator with a pure, classic MC method serves as reference solution $\tilde{Y}_{Ref.} = 95.44\%$. Note that the number of high fidelity evaluations $|\text{HF}_{Ref.}| = 26,360$ is not $|T_d| \cdot N_{MC} = 27,500$ as one could expect. The reason is that, if \mathbf{p}_i fails to fulfill the inequality for one arbitrary frequency point, this sample point is rejected without any further tests (*short-circuit evaluation*), since the inequality in (2) needs to hold for each $\omega_j \in T_d$. In order to build the GPR models, the initial training data set consists of ten random data points generated according the truncated Gaussian distribution $\mathcal{N}_T(\bar{\mathbf{p}}, \Sigma, \text{lb}, \text{ub})$ of the uncertain parameters. Only this initial training data set is the same for all GPR models. Then, the estimation procedure with Algorithm 2 is started. Every $N_{update} = 50$ MC sample points the GPR models are updated individually if there were critical sample points on them. The yield estimator is $\tilde{Y}_{GPR-H} = 95.44\%$, so we obtain the same accuracy as with pure MC. The computational effort can be reduced to $|\text{HF}_{GPR-H}| = 110 + 251 = 361$, which is a reduction by factor 73. Here, the first number refers to the offline costs, i.e. the high fidelity evaluations to build the initial surrogate model, the second number refers to the evaluation of the critical sample points.

Using, the stochastic collocation hybrid approach proposed in [8], the same accuracy was reached while the effort was $|\text{HF}_{SC-H}| = 330 + 165 = 495$ high-fidelity model evaluations. In both methods the number of training data points was chosen such that the method performs best. The higher number of offline evaluations in the stochastic collocation approach could be due to the fact that the surrogate model cannot be updated during the estimation and therefore it requires more initial training data to perform well.

4.2 Comparison with a linearization approach

In practice, often a simple linearization of the QoI is used for the MC analysis, assuming that the design parameter deviations are small enough to obtain valid results [12]. Therefore we compare the proposed GPR-Hybrid approach with linearization in the following. Linearizations means here, that we use a surrogate model, built by linear interpolation with two points in each dimension, i.e. in addition to $\mathbf{p}^0 = [p_1^0, p_2^0, p_3^0, p_4^0]^T$ we consider the four nodes

$$\mathbf{p}^k = \mathbf{p}^0 + \delta_{\mathbf{p}} \mathbf{e}_k, \quad k = 1, \dots, 4,$$

where \mathbf{e}_k is the k -th unit vector and $\delta_{\mathbf{p}} > 0$ the step size (if interpreted in the context of finite differences). Alternatively, derivative information could be used if available. These five nodes are used to create a linear approximation according to

$$\tilde{S}_{\omega_j}(\mathbf{p}^k) = \sum_{l=1}^{|\mathbf{p}^k|} (a_l \mathbf{p}_l^k) + a_{|\mathbf{p}^k|+1},$$

where $|\mathbf{p}^k|$ is the length of the vector \mathbf{p}^k and the a_l are the coefficients of the linearization. This model is setup for each frequency point ω_j and for the real and the imaginary part of the S-parameter separately. Then a MC analysis on the linear surrogate models is performed. In Figure 2 we see the results of the yield estimation for different values of $\delta_{\mathbf{p}}$. We compare this to the MC solution on the original model as reference solution and the GPR-Hybrid solution

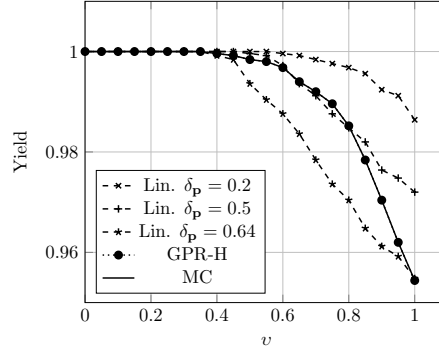


Figure 2: Comparison of different yield estimation approaches over v : Reference solution is MC which coincides with the GPR-Hybrid approach. The linearization approach is plotted for different values of the step size $\delta_{\mathbf{p}}$.

from Section 4.1. The values of the yield estimation are plotted over $v \in [0, 1]$, which is a measure of the magnitude of deviation since \mathbf{p} is (truncated) Gaussian distributed with $\mathbf{p} \sim \mathcal{N}_{\mathcal{T}}(\bar{\mathbf{p}}, v \Sigma, \mathbf{lb}, \mathbf{ub})$. For $v = 1$ we obtain the results of Section 4.1, for $v < 1$ the scaled variance decreases and the yield estimator increases until for $v = 0$ there is no uncertainty at all and the yield is $Y = 1$ since $\bar{\mathbf{p}}$ is in the safe domain. While the GPR-Hybrid solution exactly matches the reference solution, we observe considerable deviations in the linearization model for any value of $\delta_{\mathbf{p}}$ (for $v > 0.5$). These deviations decrease as expected with decreasing variance.

4.3 Lowpass Filter

We consider as industrial example a stripline lowpass filter, see Figure 3, taken from the examples library of CST Studio Suite® [12]. We consider six uncertain geometrical parameters $\mathbf{g} = [L_1, L_2, L_3, W_1, W_2, W_3]^T$ describing length and width of the single blocks. Again, we assume the uncertain parameters to follow a truncated Gaussian distribution with mean and covariance (in mm) given by

$$\bar{\mathbf{g}} = [6.8, 5.1, 9.0, 1.4, 1.4, 1.3]^T \quad \text{and} \quad \Sigma_{\mathbf{g}} = \text{diag}([0.3^2, 0.3^2, 0.3^2, 0.1^2, 0.1^2, 0.1^2]).$$

The distribution of L_1, L_2 and L_3 is truncated at $L_i \pm 3$ mm ($i = 1, 2, 3$), the distribution of W_1, W_2 and W_3 at $W_i \pm 0.3$ mm ($i = 1, 2, 3$). Since the requirement for a low pass filter is to allow low frequency signals to pass through while filtering out high frequency signals, in this example we have two performance feature specifications given by

- I.) $|S_{\omega}(\mathbf{g})| \stackrel{!}{\geq} -1 \text{ dB} \quad \forall \omega \in T_{\omega,1} = [2\pi 0, 2\pi 4] \text{ in GHz},$
- II.) $|S_{\omega}(\mathbf{g})| \stackrel{!}{\leq} -20 \text{ dB} \quad \forall \omega \in T_{\omega,2} = [2\pi 5, 2\pi 7] \text{ in GHz}.$

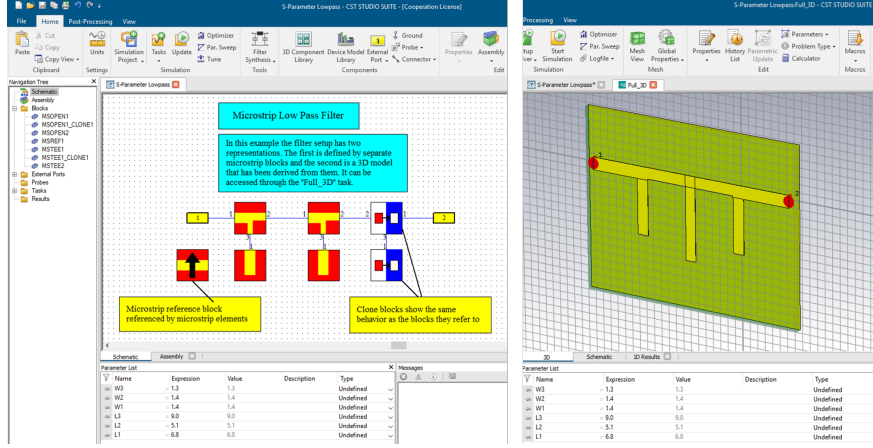


Figure 3: Lowpass filter from examples library of CST Studio Suite® [12].

According to (7), the sample size is set to $N_{MC} = 2,500$, in order to guarantee a standard deviation of the yield estimator of less than 0.01 for each size of the yield. The estimation parameters are set as before: $N_{update} = 50$, $\varepsilon_t = 0.01$ and $\gamma = 2$. Also, the kernel function and the hyperparameter settings are as in the previous example. Further we consider eight equidistant frequency points $\omega_j \in T_d$, i.e. eight GPR surrogate models are built. The evaluation of the high fidelity model is implemented by the frequency domain solver in CST Studio Suite®, using the default parameters. The mathematical model is described in [21]. An evaluation within CST calculates the S-parameter in a whole frequency range, i.e. for all considered frequency points $\omega_j \in T_d$. Therefore, with respect to this example, we consider the number of CST calls as a measure for the computational effort. For a yield estimation with a pure Monte Carlo analysis we would have a computational effort of $|CST_{Ref.}| = 2,500$ and obtain an estimated yield of $\tilde{Y}_{Ref.} = 86.56\%$.

In the GPR-Hybrid approach we use an initial training data set of 30 sample points. This means we have an offline cost of 30, because all frequency points are evaluated simultaneously in CST. Now we evaluate the N_{MC} sample points on the GPR model. If one sample point for one frequency point turns out to be a critical sample point, we evaluate this sample point for all frequency points with CST and use this information also for a possible update of the GPR model. We have a total of 429 critical sample points. This results in a computational effort of $|CST_{GPR-H}| = 30 + 429 = 459$ and a yield of $\tilde{Y}_{GPR-H} = 86.56\%$. Thus, with the GPR-Hybrid approach we can reduce the computational effort by a factor more than 5 compared to pure Monte Carlo, while maintaining the same accuracy. The lower savings in computational effort compared to the previous example of the waveguide is due to the fact that it is a more complex example on the one hand, but on the other hand also due to the simultaneous evaluation of all frequency points, because often a sample point is not critical for all frequency points.

Figure 4 shows the number of CST evaluations over the number of evaluated MC sample points. For 0 evaluated MC sample points the offline costs are plotted, then the critical sample points after every 50 evaluated MC sample points. As expected, the number of critical sample points is quite high in the beginning, but after three model updates the GPR model is improved so that the number of critical sample points remains at a low constant level until the end.

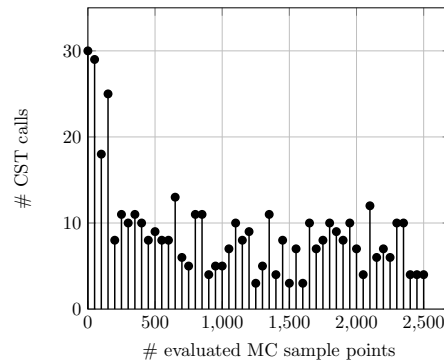


Figure 4: Number of CST calls during the yield estimation process.

5 Conclusions

A hybrid approach combining the efficiency of surrogate based approaches and the reliability and accuracy of the classic Monte Carlo method has been proposed. As surrogate model Gaussian Process Regression has been introduced and its variance estimator was used as error indicator. Numerical results show that the computational effort can be significantly reduced while maintaining accuracy. This allows yield estimation in a reasonable time without the need for high performance computers as it would be the case with a pure Monte Carlo analysis. Future research will focus on embedding the presented yield estimation methods in yield optimization. Furthermore, non greedy strategies for the learning from critical sample points could be investigated.

Acknowledgements

The work of Mona Fuhrländer is supported by the Excellence Initiative of the German Federal and State Governments and the Graduate School of Computational Engineering at TU Darmstadt. The authors would like to thank Frank Mosler of Dassault Systèmes Deutschland GmbH for the fruitful discussions regarding the setup of the industrial example.

References

- [1] Graeb, H.E.: Analog Design Centering and Sizing. Springer, Dordrecht (2007)
- [2] Hammersley, J.M., Handscomb, D.C.: Monte Carlo Methods. Methuen & Co Ltd, London (1964)
- [3] Rao, C.R., Toutenburg, H.: Linear Models: Least Squares and Alternatives, 2nd edn. Springer, New York (1999)
- [4] Rasmussen, C.E., Williams, C.K.I.: Gaussian Processes for Machine Learning. The MIT Press, Cambridge (2006)
- [5] Babuška, I., Nobile, F., Tempone, R.: A stochastic collocation method for elliptic partial differential equations with random input data. *SIAM J. Numer. Anal.* **45**(3), 1005–1034 (2007). doi:10.1137/100786356
- [6] Li, J., Xiu, D.: Evaluation of failure probability via surrogate models. *J. Comput. Phys.* **229**(23), 8966–8980 (2010). doi:10.1016/j.jcp.2010.08.022
- [7] Butler, T., Wildey, T.: Utilizing adjoint-based error estimates for surrogate models to accurately predict probabilities of events. *Int. J. Uncert. Quant.* **8**(2), 143–159 (2018). doi:10.1615/Int.J.UncertaintyQuantification.2018020911
- [8] Fuhrländer, M., Georg, N., Römer, U., Schöps, S.: Adaptive Newton-Monte Carlo for efficient and fully error controlled yield optimization. Preprint, Cornell University (2019)
- [9] Bect, J., Li, L., Vazquez, E.: Bayesian subset simulation. *SIAM/ASA J. UQ* **5**(1), 762–786 (2017). doi:10.1137/16m1078276
- [10] Xiao, S., Oladyshkin, S., Nowak, W.: Reliability analysis with stratified importance sampling based on adaptive kriging. *Reliability Engineering & System Safety* **197**, 106852 (2020)
- [11] Zhang, J., Taflanidis, A.A.: Accelerating mcmc via kriging-based adaptive independent proposals and delayed rejection. *Computer Methods in Applied Mechanics and Engineering* **355**, 1124–1147 (2019)
- [12] Dassault Systèmes Deutschland GmbH: CST Studio Suite® (2018). www.3ds.com
- [13] Jackson, J.D.: Classical Electrodynamics, 3rd edn. Wiley & Sons, New York (1998). doi:10.1017/CBO9780511760396
- [14] Nédélec, J.C.: Mixed finite elements in R3. *Numer. Math.* **35**(3), 315–341 (1980). doi:10.1007/BF01396415
- [15] Monk, P.: Finite Element Methods for Maxwell’s Equations. Oxford University Press, Oxford (2003)
- [16] Cohen, A.C.: Truncated and Censored Samples: Theory and Applications, pp. 1–303 (2016)
- [17] Giles, M.B.: Multilevel Monte Carlo methods. *Acta. Num.* **24**, 259–328 (2015). doi:10.1017/S09624929
- [18] Gustavsen, B., Semlyen, A.: Rational approximation of frequency domain responses by vector fitting. *IEEE Trans. Power Deliv.* **14**(3), 1052–1061 (1999). doi:10.1109/61.772353
- [19] Pedregosa, F., Varoquaux, G., Gramfort, A., Michel, V., Thirion, B., Grisel, O., Blondel, M., Prettenhofer, P., Weiss, R., Dubourg, V., Vanderplas, J., Passos, A., Cournapeau, D., Brucher, M., Perrot, M., Duchesnay, E.: Scikit-learn: Machine learning in Python. *Journal of Machine Learning Research* **12**, 2825–2830 (2011)
- [20] Loukrezis, D.: Benchmark models for uncertainty quantification. GitHub (2019). https://github.com/dlouk/UQ_benchmark_models/tree/master/rectangular_waveguides/debye1.py

- [21] Eller, M., Reitzinger, S., Schöps, S., Zaglmayr, S.: A symmetric low-frequency stable broadband Maxwell formulation for industrial applications. *SIAM J. Sci. Comput.* **39**(4), 703–731 (2017). doi:10.1137/16M1077817